

Article

Morphology of Detrital Zircon as a Fingerprint to Trace Sediment Provenance: Case Study of the Yangtze Delta

Wei Yue ^{1,2,*}, Xiyuan Yue ³, Lingmin Zhang ², Xianbin Liu ⁴ and Jian Song ⁴

¹ School of Geography, Geomatics and Planning, Jiangsu Normal University, Xuzhou 221116, China

² State Key Laboratory of Marine Geology, Tongji University, Shanghai 200092, China

³ Shandong Key Laboratory of Eco-environmental Science for Yellow River Delta, Binzhou University, Binzhou 256603, China

⁴ School of Resources and Environmental Engineering, Ludong University, Yantai 264025, China

* Correspondence: yuewei@jsnu.edu.cn

Received: 21 June 2019; Accepted: 15 July 2019; Published: 17 July 2019



Abstract: Deltaic areas and marginal seas are important archives that document information on regional tectonic movement, sea level rise, river evolution, and climate change. Here, sediment samples from boreholes of the Yangtze Delta and the modern Yangtze drainage were collected. A quantitative analysis of detrital zircon morphology was used to discuss the provenance evolution of the Yangtze Delta. This research demonstrated that a dramatic change in sediment provenance occurred in the transition from the Pliocene to Quaternary. Zircon grains in the Pliocene sediments featured euhedral crystals with large elongation (>3 accounted for 13.2%) and were closely matched to tributary samples in the Lower Yangtze (>3 accounted for 11.3%), suggesting sediment provenance from the proximal river basin. However, most detrital zircon grains of the Quaternary samples exhibited lower values of elongation and increased roundness (rounded grains were 9.4%), which was similar to those found in the modern Yangtze mainstream (rounded grains were 12.5%) and the middle tributaries (rounded grains were 7.0%). The decrease in zircon elongation and improvement of its roundness in the Quaternary strata implied that the Yangtze Delta received sediments of different provenance that originated from the Middle-Upper Yangtze basin due to the uplift of the Tibetan Plateau. Statistical analysis of detrital zircon morphology has proven useful for studying the source-to-sink of sediments.

Keywords: sediment provenance; zircon morphology; Quaternary; the Yangtze Delta; elongation

1. Introduction

Large river deltas and marginal seas receive large quantities terrigenous sediments, making them ideal sites for the study of source-to-sink systems and land-sea interaction on multiple spatiotemporal scales [1–3]. In order to carry out source identification effectively, multiple technical means including bulk-sediment geochemistry, heavy minerals analysis, and single-mineral in situ analysis are widely applied [4–6]. Regarded as one of the most stable minerals in sediments, zircon has a strong resistance to burial diagenesis and chemical weathering [4,7]. Moreover, it can be easily separated from the sediment. Several researchers have used the geochemistry of zircon to trace sediment provenance and made substantial achievements [8–10]. However, it is very expensive to analyse a large number of samples. In addition, scholars are advised to integrate multiple techniques in order to avoid misleading interpretations caused by a single research method [11,12]. Apart from its geochemistry, the features of zircon morphology including its crystal population, elongation, and roundness are feasible to

intuitively determine zircon parent rocks and are potential fingerprints to be applied in sediment provenance analysis [13–17].

Serving as an important depocenter of the Eastern China, the Yangtze Delta has preserved valuable information on sediment sources related to landform and river evolution [5,18,19]. Using different methods of clay mineral analysis, geochemistry, magnetic properties, single mineral geochronology (zircon, monazite age spectra), previous studies have identified a significant change in sediment provenance at the Pliocene-Quaternary transition [20–23]. However, sediment provenance evolution in the deltaic area is still controversial [22]. There is neither a consensus about the exact source of the Pliocene strata in the Yangtze Delta nor about the time when the Upper Yangtze sediments arrived at the delta. Different studies proposed that the Upper Yangtze sediment arrived either early in the Pliocene [21,24], in the Early-Middle Pleistocene [22,23,25–27], or later in the late Pleistocene [28,29]. For these previous studies, only one borehole was used to represent the entire area of the Yangtze Delta, which may have resulted in different interpretations due to the limitations of the different methods. This is not only because of the vast area of Yangtze Delta but also because of its complex sedimentary strata.

In order to extract the exact sediment provenance, several boreholes in different regions of the study area should be systematically analysed and compared to potential source sediments within the Yangtze drainage. In addition, the bottom strata of the Yangtze Delta were compacted and slightly affected by diagenesis [23]. High abundances of stable minerals (ilmenite, zircon, and tourmaline) and altered minerals (limonite, leucoxene) indicate strong chemical weathering in the Pliocene sediments [27]. For these semi-consolidated sediments, reliable discrimination indicators should be adapted for sediment provenance analysis. As one of the ultrastable mineral, zircons are ideal archives to document the original provenance signal. However, insufficient attention has been given to the zircon morphology analysis. In the Yangtze Delta, zircon morphology and chronology was studied to trace the sediment provenance evolution [21,27]. With respect to the zircon morphology analysis in the Yangtze Delta, the potential source areas were not involved. Moreover, the previous study was done on small amounts of zircon grains by using traditional methods (optical microscope observation) [27].

In the present study, three deep boreholes, LQ11, LQ19, and LQ24, were taken from different regions of the Yangtze Delta, and their burial depth is 302.2 m, 322.2 m and 399.8 m, respectively. In order to compare core samples with potential source areas, surface sediment samples of the mainstream and tributaries in the Middle-Lower Yangtze and Qiantang River were collected. In order to ensure the reliability of the result, sufficient zircon grains were studied. The zircon morphology in both core sediments and river surface sediment samples was measured by scanning the electron microscope with the aim to identify the sediment provenance of the Yangtze Delta since the Pliocene.

2. Geological Setting

2.1. Yangtze River Drainage Basin

The Yangtze River is the longest (>6300 km) in Asia and covers a vast basin area of 1.8 million km² [30]. Originating at the Tibet Plateau, it pours 900×10^9 m³ of fresh water and 390×10^6 tons of sediments per year into the East China Sea [31]. In recent years, the Yangtze River has experienced a dramatic reduction in sediment flux, and its annual average sediment discharge decreased to $\sim 120 \times 10^6$ tons after 2002 when the Three Gorges Dam was completed [31].

The Yangtze River drainage is divided into five tectonic units, including the Qamdo Block, the Songpan-Garze terrane, the Yangtze Craton, the Qinling-Dabie orogenic belts, and the Cathaysia Block [32]. Based on its topographical features, the upper, middle and lower reaches of the Yangtze River drainage have different characteristics, as shown in Figure 1. The upper reaches span from its headwater to the Three Gorges near Yichang City [33]. This section has a drainage area of approximately 1.0×10^6 km² and occupies a length of >4000 km. The Upper Yangtze is featured by steep mountains and deep canyons and comprises various tectonic units and different kinds of rocks [32,33]. These

rocks were formed during various geological time including the Archaean, Palaeozoic, Mesozoic, and Cenozoic [34]. The Middle Yangtze flows from the Three Gorges to Hukou County in the Jiangxi Province. The Yangtze mainstream of this section has a length of 950 km and covers a drainage area of approximately 0.7×10^6 km². This area is featured by hills and meandering platforms Figure 1. In the Middle Yangtze, the Palaeozoic sedimentary rocks, Archaean-Cenozoic metamorphic rocks and Mesozoic-Cenozoic igneous rocks are widely distributed [32]. The Lower Yangtze extends from Hukou until the estuary in Shanghai. Its mainstream river length is about 1000 km but only occupies a drainage area of roughly 0.1×10^6 km². The lower reaches host large blocks of Mesozoic intermediate-acidic igneous rocks.



Figure 1. Sampling locations of the surface sediment in the Modern River and borehole sediment in the Yangtze Delta. R. = River, sl = Sampling location, YZ-YC = Yangtze mainstream near Yichang City, YZ-TL = Yangtze mainstream near Tongling City, YZ-SH = Yangtze mainstream near Shanghai City, GJ = Ganjiang River, XJ = Xiangjiang River, HJ = Hanjiang River, QYJ = Qingyijiang River, SYJ = Shuiyangjiang River, TX = Tiaoxi River, XAJ = Xinanjiang River, QTJ = Qiantang River.

2.2. The Stratigraphy and Chronology of the Yangtze Delta

The Yangtze Delta has a thickness of 200–400 m of unconsolidated sediment stratum, as shown in Figure 2. Based on palaeomagnetic dating results, the bottom stratum of the Yangtze Delta was formed since the Neogene Period [23]. In general, the magnetostratigraphic boundary between the Matuyama and Gauss epochs (M/G) lies at core depths of 160–300 m, dividing the Pliocene from the Pleistocene [23]. In our study, the M/G boundary of Cores LQ11, LQ19, and LQ24 was located at burial depths of 252 m, 278 m, and 337 m, respectively Figure 2. Detailed stratigraphic chronology was deciphered by [23], [22], and [27].

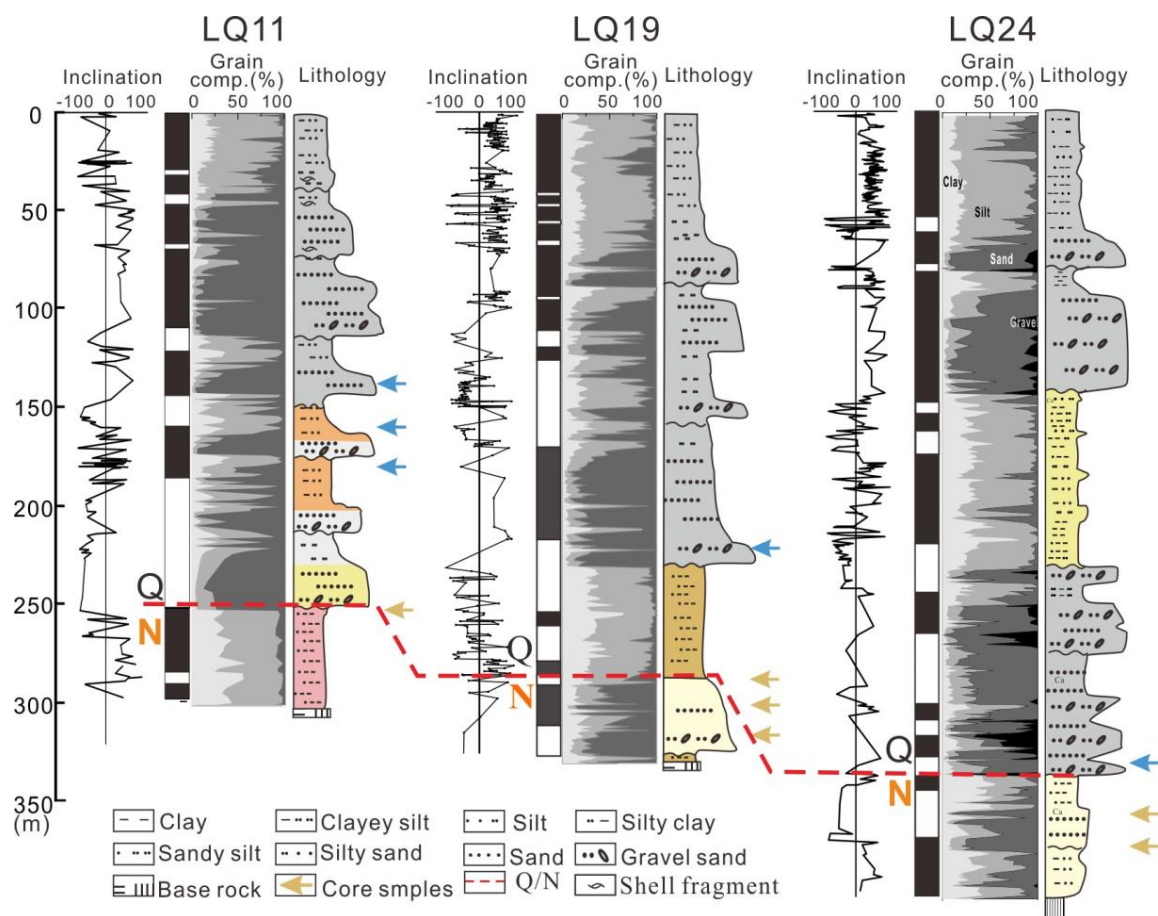


Figure 2. Sediment sampling depth and stratigraphy of Cores LQ11, LQ19, and LQ24. Comprehensive stratigraphic information on the strata of the Yangtze Delta includes sedimentary facies, polarity epoch, and sediment composition. Q = Quaternary, N = Pliocene. The red dotted line represents the Pliocene-Pleistocene boundary. Logs of LQ11, LQ19, and LQ24 are modified after [23], [22], and [27], respectively.

The late Cenozoic stratigraphy of the Yangtze Delta has five to six sedimentary cycles [35]. The Pliocene strata have a thickness of <100 m and directly overlie the late Mesozoic-Cenozoic magmatic bedrocks with a weathering unconformity. These strata comprise several sedimentary sequences that mainly contain clayey silt and vermiculated stiff clay. Each sequence shows a fining-upward with medium-fine sand at the bottom and clay at the top. The Pliocene sediments contain a number of iron-manganese nodules and calcareous concretions. Furthermore, coarse sediments of gravel sand can be found, with diameters ranging from 2–50 mm.

The Quaternary strata (50–300 m) of the Yangtze Delta overlie the Pliocene strata with a distinct weathering unconformity in Figure 2. The sediment in this layer is mainly composed of silt, fine sand and gravel, which display sedimentary features typical for fluvial systems [35]. The layer contains several fining-upward sedimentary sequences in which dark-grey sand (ca. 5 m thick) is at the bottom and grey silty clay (ca. 5 m thick) is at the top. The Quaternary strata are complex, and are featured by the river channel, tidal river, estuarine, lacustrine, and mud tidal flat facies [18]. Foraminifera and shell debris began to occur in the Mid-Late Quaternary sediment, indicating marine transgressions in this area [36].

3. Materials and Methods

In the present study, sediment samples were taken from two areas: The sink and the source regions, as shown in Figure 1. In the sink area, three continuous boreholes (LQ11, LQ19, and LQ24)

that span from the Holocene, the Pleistocene, and the Pliocene until the bedrock, were collected in Figure 1. A total of 11 borehole sediment samples were selected for the morphology analysis of detrital zircon. The sediment sampling was based on the paleomagnetic dating results in order to ensure that samples were located at the Pliocene-Quaternary transition. Detailed strata information including paleomagnetic dating, micropaleontology, and sedimentary facies were documented in [23], [22], and [27].

In the potential source area, a total of 11 surface sediments were collected from the modern Yangtze mainstream, tributaries of the Middle-Lower Yangtze, and the Qiantang River in Figure 1. All of these river sediments were collected from the floodplain or central bars. For each sample, more than 2 kg sediments were taken with a clean wooden spoon.

To analyse the morphology of detrital zircon grains, the size fraction of very fine sand (63–125 μm) was chosen because it contained a high percentage of heavy minerals in the Yangtze sediment, which allowed for the relatively easy optical observation of mineral grains [3]. The separation of heavy minerals abided by the standard procedures described by [37]. Firstly, the very fine sand fraction was separated and wet-sieved through 63 μm and 125 μm sieves to rinse off the clay, silt, and the coarse fractions. After being dried at 40 $^{\circ}\text{C}$, the fine sand was separated with a sodium polytungstate solution (density of 2.88 g/cm^3) at 20 $^{\circ}\text{C}$. After the heavy liquid separation process, heavy minerals were then used for zircon collection with a Frantz magnetic separator. Detrital zircon grains were randomly picked under a stereoscopic microscope, identified, and examined under a polarizing microscope. Finally, the zircon grains were coated with carbon and photographed by a scanning electron microscope (XL-30 ESEM from Philips) to carry out the morphology analysis. The zircon analysis was performed in the State Key Laboratory of Marine Geology, Tongji University (Shanghai, China). The length and width of each zircon grain were measured by the software Image J, and the elongation was calculated by the ratio of length to width.

A total of 1642 detrital zircon grains with unbroken crystal shape were analysed with respect to their morphology, including elongation (length-to-width) and the degree of roundness. Although several authors have investigated the morphology of zircon crystal grains, there is no agreement concerning the definition or classification of roundness [13,38]. There are several reasons for this, e.g., certain zircons lose their outer layers and then appear nearly fresh again, making it difficult to distinguish the subangular grains from the subrounded ones. Thus, these two types are combined into one type. In this study, three types of roundness including angular, subangular, and rounded were set according to the standard classification of roundness [39]. For the elongation (the length-width ratio) analysis, four groups were identified including <2, 2–3, 3–4, and >4.

4. Results

4.1. Detrital Zircon Morphology Features of Core Sediment in the Yangtze Delta

Based on the characteristic vertical distribution of detrital zircon morphology in Cores LQ11, LQ19, and LQ24, two different zones were identified in Figures 3 and 4. The boundary of these two zones was located in the Pliocene-Pleistocene boundary.

The Pliocene samples:

In this zone, the elongation of zircon grains ranged from 1.0 to 4.8. Based on the elongation classification, three samples contained four groups and the other three samples had three types, as shown in Table 1. Approximately half of the detrital zircon grains from the Pliocene strata showed the elongation between two to three in Figure 3. In addition, the small elongation of <2 accounted for around 40%, ranging from 37.7% to 44.0% in Table 1. Furthermore, the percentage of the large elongation (>3) was 13.2% on average, ranging from 8.0% to 15.8%.

Similar to the vertical variation of the elongation, the roundness of zircon in the Pliocene samples was generally poor (angular-subangular). In these samples, angular and subangular crystals accounted

for average proportions of 79% and 20%, respectively. Rounded zircon grains (only 1%) were rarely observed in this zone in Figure 4.

The Quaternary samples:

In contrast to the Pliocene samples, the detrital zircon with a small elongation ratio increased in the Quaternary samples, as shown in Figure 3. The proportion of the small elongation group (<2) increased significantly up to nearly two thirds, ranging from 56.1% to 72.6%. Elongations between two and three were found in 22.6% to 37.3% of the five Quaternary samples. Moreover, the proportion of the large elongation ratio (>3) accounted for up to 4.8% on average, ranging from 1.3% to 10.5%.

Well-rounded zircon grains were more abundant in the Quaternary samples than in the Pliocene samples, as shown in Figure 4. Although the angular zircon grains were still prevalent in the Quaternary samples, subangular and rounded zircon grains increased significantly. In this zone, zircon grains with angular, subangular, and rounded shapes averaged 43.9%, 46.7%, and 9.4%, respectively.

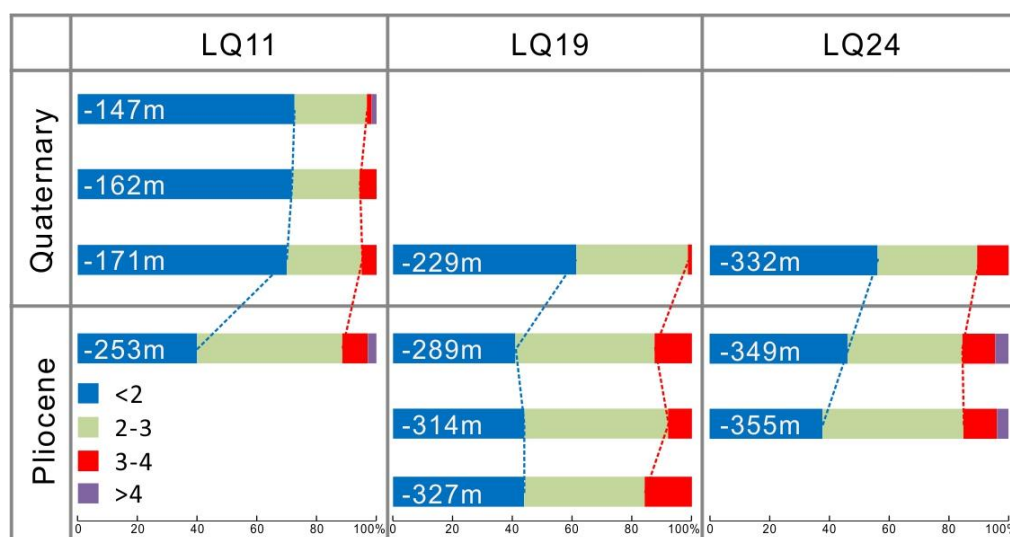


Figure 3. Features of detrital zircon elongation in the core sediment of LQ11, LQ19, and LQ24 in the Yangtze Delta.

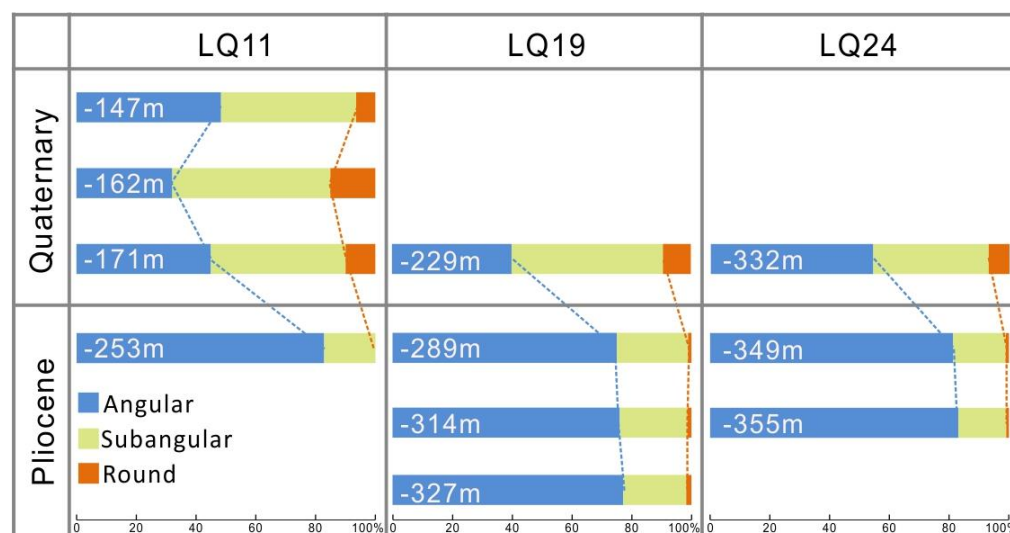


Figure 4. Features of detrital zircon roundness in the core sediment of LQ11, LQ19, and LQ24 in the Yangtze Delta.

Table 1. Elongation and roundness statistics of detrital zircon in modern rivers and core samples of the Yangtze Delta. Q = Quaternary, N = Pliocene, NYZD = North Yangtze Delta, MYZD = Middle Yangtze Delta, SYZD = South Yangtze Delta, YZ-M = Yangtze mainstream, TM-YZ = Modern tributaries of the Middle Yangtze, TL-YZ = Modern tributaries of the Lower Yangtze. Please see Figure 1 for the explanation of the abbreviations of some place names.

Location	Samples (No)	Elongation (%)				Roundness (%)			Standard Deviation			
		<2	2–3	3–4	>4	>3	Angular	Subangular	Rounded	Length	Width	Elongation
SYZD	LQ11-Q-147 m (63)	71.4	25.4	1.6	1.6	3.2	47.6	46.1	6.3	39.6	11.6	0.5
	LQ11-Q-162 m (52)	71.1	23.1	5.8	0.0	5.8	32.7	51.9	15.4	35.6	10.3	0.6
	LQ11-Q-171 m (40)	70.0	25.0	5.0	0.0	5.0	45.0	45.0	10.0	37.0	14.3	0.5
	LQ11-N-253 m (35)	40.0	48.6	8.6	2.9	11.5	82.9	17.1	0.0	41.0	18.8	0.7
MYZD	LQ19-Q-229 m (75)	61.3	37.3	1.3	0.0	1.3	40.0	50.7	9.3	33.5	19.6	0.5
	LQ19-N-289 m (88)	40.9	46.6	12.5	0.0	12.5	75.0	23.9	1.1	39.1	16.3	0.6
	LQ19-N-314 m (75)	44.0	48.0	8.0	0.0	8.0	76.0	22.7	1.3	53.6	19.1	0.5
	LQ19-N-327 m (57)	43.9	40.4	15.8	0.0	15.8	77.2	21.1	1.8	69.6	20.0	0.7
NYZD	LQ24-Q-332 m (57)	56.1	33.3	10.5	0.0	10.5	54.4	38.6	7.0	39.6	17.2	0.6
	LQ24-N-349 m (91)	46.2	38.5	11.0	4.4	15.4	81.3	17.6	1.1	51.7	15.8	0.8
	LQ24-N-355 m (106)	37.7	47.2	11.3	3.8	15.1	83.0	16.0	0.9	53.1	17.7	0.7
YZ-M	YZ-YC (101)	68.3	28.7	3.0	0.0	3.0	53.5	35.6	10.9	36.2	15.4	0.5
	YZ-TL (77)	58.4	36.4	5.2	0.0	5.2	53.2	35.1	11.7	33.0	15.7	0.6
	YZ-SH (102)	59.8	35.3	4.9	0.0	4.9	44.1	41.2	14.7	41.9	13.9	0.6
TM-YZ	GJ (77)	54.5	41.6	3.9	0.0	3.9	51.9	40.3	7.8	45.8	18.4	0.5
	XJ (69)	65.2	33.3	1.4	0.0	1.4	43.5	50.7	5.8	38.1	16.9	0.5
	HJ (55)	60.0	38.2	1.8	0.0	1.8	45.5	47.3	7.3	32.8	12.3	0.5
TL-YZ	TX (64)	40.6	48.4	9.4	1.6	11.0	89.1	10.9	0.0	43.3	12.5	0.6
	QYJ (103)	45.6	45.6	8.7	0.0	8.7	75.7	22.3	1.9	37.0	11.4	0.6
	XAJ (77)	33.8	53.2	7.8	5.2	13.0	72.7	23.4	3.9	41.7	14.2	0.7
	SYJ (71)	53.5	36.6	7.0	2.8	9.8	46.5	39.4	14.1	39.7	13.5	0.7
Qiantang	QTJ (107)	35.5	50.5	9.3	4.7	14.0	71.0	26.2	2.8	44.8	11.5	0.9

4.2. Detrital Zircon Morphology Characteristics of the Modern Rivers

Modern river data showed that the elongation and roundness of zircon were significantly different between the tributaries and the Yangtze mainstream, as shown in Figure 5. The Lower Yangtze tributary and Qiantang River contained four elongation groups and were mainly composed of the groups of <2 and 2–3, representing 41.5% and 47.2% on average, respectively. The average proportion of large elongation (>3) was about 10%.

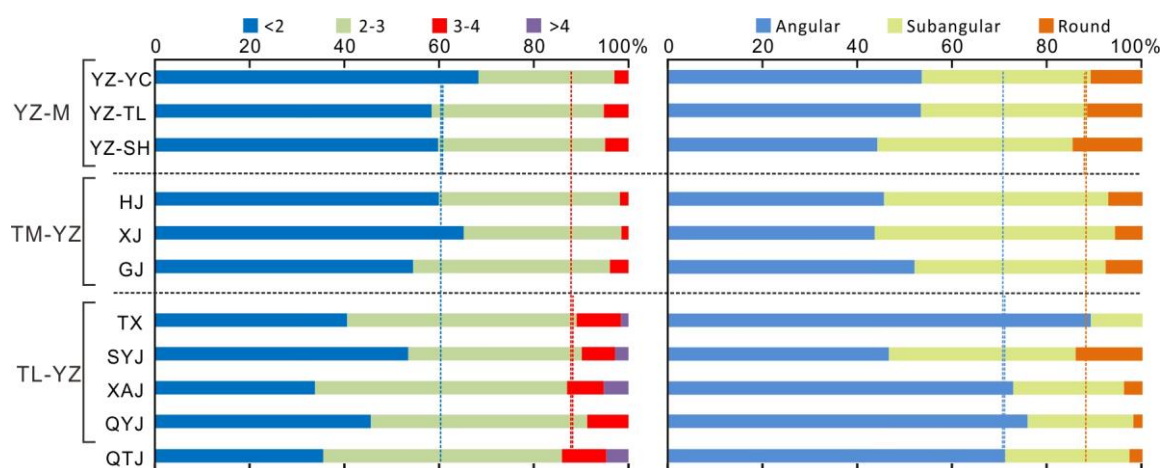


Figure 5. Zircon elongation and roundness of surface sediment samples in the Yangtze drainage and Qiantang River. YZ-M = Yangtze mainstream, TM-YZ = Tributaries of the Middle Yangtze, TL-YZ = Tributaries of the Lower Yangtze. Please see Figure 1 for the explanation of the abbreviations of some place names.

The sediment groups of the Yangtze mainstream and the Middle Yangtze tributaries were indistinguishable from each other with respect to their average elongation and roundness. The Yangtze mainstream yielded zircon elongation groups <2, 2–3, and 3–4, whereas it lacked groups >4. The average proportion of the elongation group of <2 was 62.5%, and the large elongation of >3 decreased to only 4.3%. On the other hand, the average percentage of angular, subangular, and rounded zircon in the mainstream accounted for 50.0%, 37.5% and 12.5%, respectively; while these zircon types averaged 71.1%, 24.6%, and 4.3% in the Lower Yangtze tributaries. However, samples of the Middle Yangtze tributaries were characterised by shorter and less rounded detrital zircon grains, as shown in Figure 5. The well-rounded zircon grains accounted for 7.0% on average. The average proportion of the elongation group of <2 was 62.2%, and the large elongation of >3 was only 4.4%.

5. Discussion

5.1. Sediment Provenance of the Yangtze Delta in the Pliocene

For different rock types including magmatic, metamorphic, and sedimentary rocks, zircon grains developed into various crystal shapes due to different crystallization environment conditions such as temperature, pressure, pH value, oxygen fugacity, and so on [40,41]. Previous studies demonstrated that zircon is featured by slender crystals in high-level granites and acid volcanic rocks, but its crystal shapes generally are characterised by stunted and stubbed shapes in the sedimentary and low-grade metamorphic rocks [40–42]. Thus, the elongation of zircon grains that are not too round is always used as an index to reflect the crystallisation velocity and temperature [43,44].

The present study shows that the morphological features of detrital zircon grains were different between samples from the Pliocene and the Quaternary strata in the Yangtze Delta, as shown in Figure 6. Towards the bottom of LQ11, LQ19, and LQ24, zircon grains are characterised by large elongation (>3) and poor roundness, implying that their source rocks may simply be igneous sources that have not

been recycled. The elongation group of 2–3 accounted for 44.7% of the total zircon grains, and the large elongation group (>3) accounted for 13.2% on average in Table 1. Compared with potential source sediments, the average percentage of these two elongation groups was 47.2% and 11.3% in tributaries of the Lower Yangtze, shown in Table 1, which matched with the sediment samples of the Pliocene, as shown in Figures 3–5.

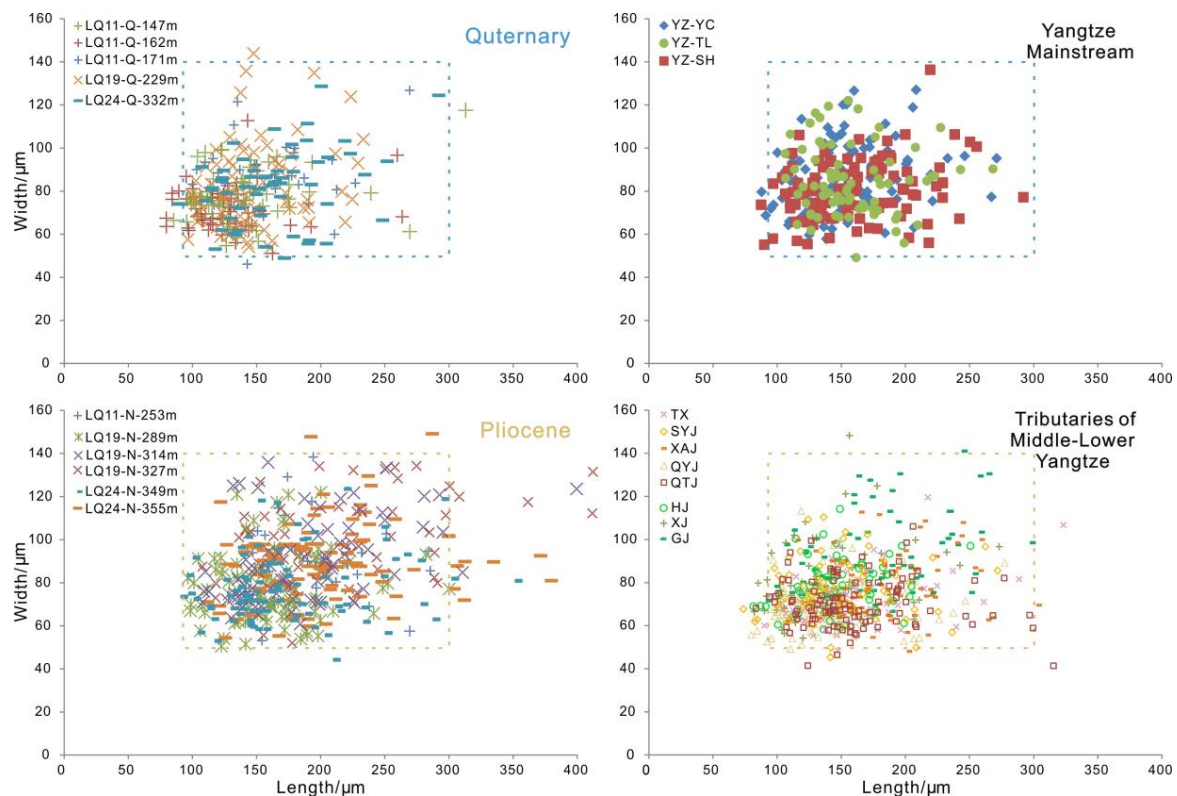


Figure 6. Length and width statistics of detrital zircon in the modern river sediment and core sediment of LQ11, LQ19, and LQ24. Q = Quaternary, N = Pliocene. Please see Figure 1 for explanation of the abbreviations of capital letters.

Further statistical data showed that slender zircon grains (length >300 μm) were observed in the Pliocene samples as well as in the modern tributaries of the Lower Yangtze, shown in Figures 6 and 7. However, such slender zircon grains were almost absent in the mainstream and tributaries of the Middle Yangtze, as shown in Figure 6. These euhedral zircon grains with the large elongation indicate volcanic and granitic source rocks that are distributed in the Lower Yangtze basin and southwestern Zhejiang Province [34]. Previous heavy mineral analysis documented high contents of ilmenite, zircon, and tourmaline in the Pliocene strata, which also suggested that the potential sources were intermediate-acid igneous rocks in the proximal basin [27,28].

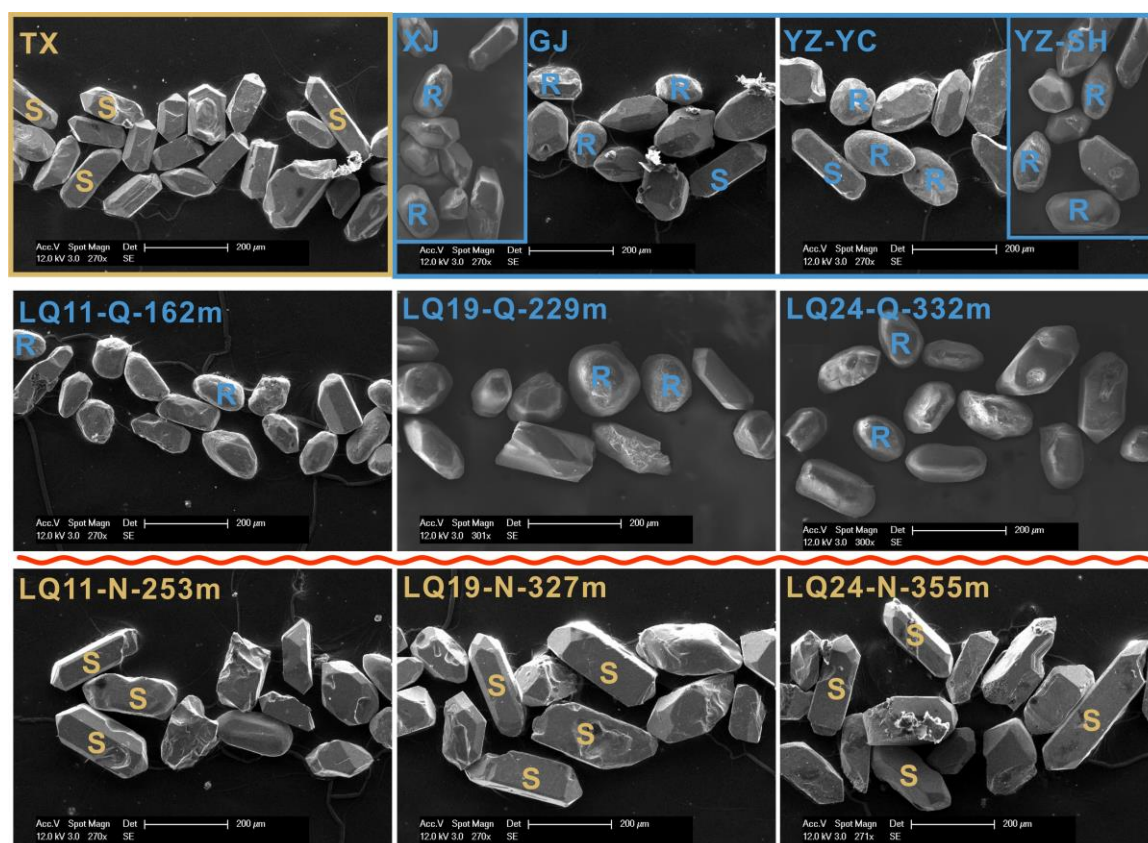


Figure 7. Zircon morphology of the Yangtze Delta and Modern River measured by a scanning electron microscope. S = Slender, R = Rounded, Q = Quaternary, N = Pliocene. In the Pliocene sediment of the Yangtze Delta, zircon grains show angular-subangular euhedral crystals, which is similar to that of the local rivers. In the Quaternary samples, the increase of the rounded and stubbed zircon is similar to the Yangtze mainstream and Middle tributaries. Please see Figure 1 for explanation of the abbreviations of capital letters.

The Pliocene samples were similar to those of the Lower Yangtze tributaries with respect to their elongation and roundness, as shown in Figure 7. The angular and subangular zircon grains accounted for average proportions of 79% and 20%, while rounded zircon grains represented only 1% in Figure 4. The lower reaches of the Yangtze host large blocks of Mesozoic intermediate-acidic igneous rocks. Other types of metamorphic and sedimentary rocks are distributed sporadically.

In the Neogene Period, the depocenter of the study area was located in the northwest of the Yangtze Delta (North Jiangsu Basin) in Figure 8. Previous studies showed that the elevation of the modern Yangtze estuary region was relatively high during that time [29,45]. Moreover, due to the low deposition rate in the study area [45], detritus had enough time to contact with the atmosphere, and more altered minerals were formed under the strong chemical weathering conditions. Detrital mineral analysis demonstrated that the Pliocene sediments were featured by abnormally high contents of limonite (ca. 30%), leucoxene, zircon, tourmaline, and extremely low levels of amphibole (5%) [27]. Controlled by the regional geologic structure, sediment sources of the study area lay in the proximal area of the southwestern Zhejiang Province, and the Zhe-Min Uplift, as shown in Figure 8. The detrital zircon U-Pb age spectra of the Pliocene sediments indicated that they were mainly composed of Cretaceous ages, which suggested proximal sources from the middle-lower reaches of the Yangtze [21,46].

In general, the features of the zircon elongation and roundness in the Pliocene sediment of the Cores LQ11, LQ19, and LQ24 closely matched with samples of the tributaries of the Lower Yangtze. This implied that the sediment provenance of the Yangtze Delta before the Quaternary was merely from the proximal basin where magmatic rocks were widely distributed.

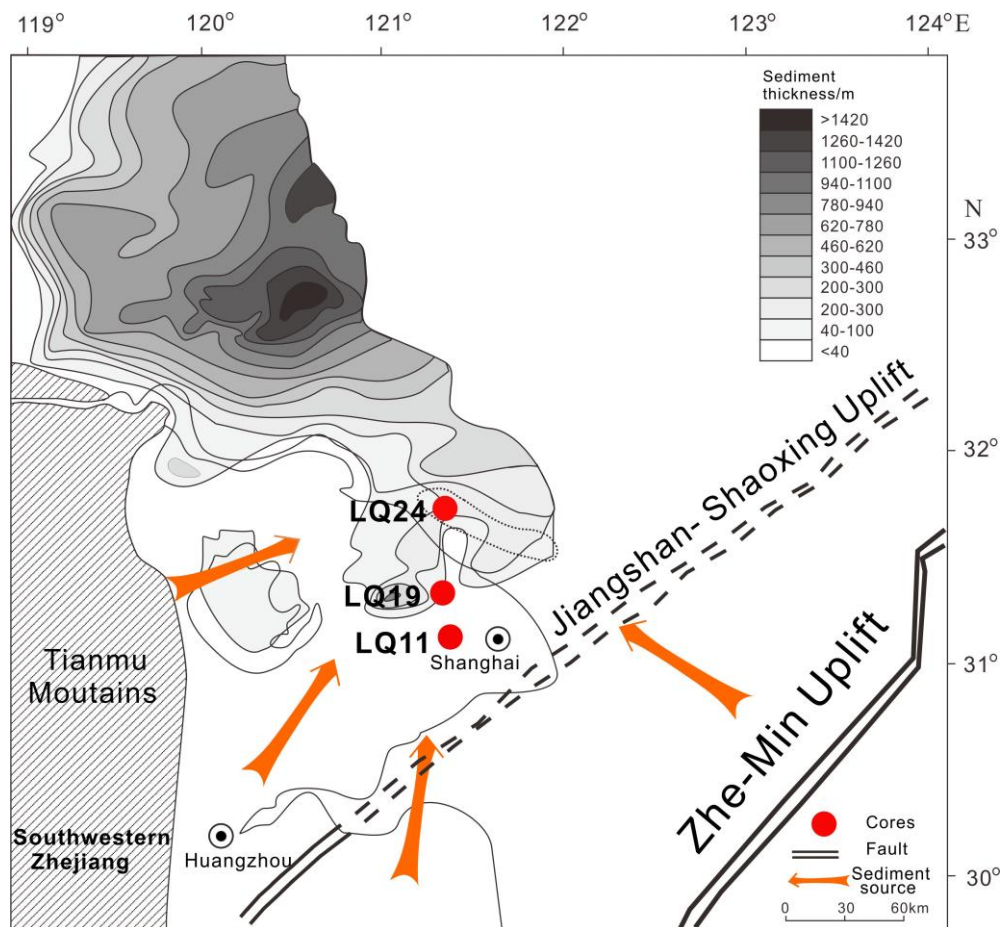


Figure 8. Sediment sources of the Yangtze Delta in the Pliocene. The contours of the sediment were modified after [45].

5.2. Sediment Provenance Change in the Yangtze Delta during the Quaternary

Contrary to the Pliocene sediment samples, the zircon morphology of the Quaternary samples was dominated by the small elongation group of <2 in Figures 3 and 7. According to the elongation statistic, the small elongation group represented approximately two thirds, while the large elongation group of >3 only accounted for 4.8% on average. The percentage of the large elongation group was about one third of the Pliocene samples and similar to that of the Yangtze mainstream (4.3% on average) and the Middle Yangtze tributaries (4.4% on average). With respect to roundness, well-rounded zircon grains occurred much more frequently in the Quaternary samples than in the Pliocene and accounted for 9.4% on average, which matched well with the sample from the Yangtze mainstream (12.5%) and was a little higher than the sample from the Middle Yangtze tributaries (7.0%) in Figures 4 and 7.

The increase of zircon grains with small elongation in the Quaternary strata can be correlated to a multitude of potential source rocks. As mentioned above, slender zircon grains often originate from intermediate-acid igneous rocks such as those of granitic and acid volcanic genesis, while stubbed shapes are from the sedimentary and low-grade metamorphic rocks. Previous studies have documented that the Middle-Upper Yangtze basin covers different rock types such as sedimentary, metamorphic, and igneous rocks [32]. The sediment source shift not only affected zircon elongation but also had an effect on zircon roundness. Well-rounded zircon grains increased significantly after the Quaternary, as shown in Figure 7. Zircon roundness can be improved by physical abrasion after long-distance transport and recycling [15,47–49]. The detrital zircon age spectra of the Quaternary sediments showed multiple peaks with higher abundance of the Neoproterozoic and Paleoproterozoic, which further implied that the sediments of the Yangtze Delta likely originated from the Tibetan Plateau [21].

Therefore, a sharp increase in rounded and stubbed zircon in the Quaternary samples from the Yangtze Delta indicated a new sediment provenance from the Middle-Upper Yangtze in Figure 9. Sediment provenance shifted from the proximal area to multiple regions in the Middle-Upper Yangtze can be interpreted as the accelerated tectonic subsidence in East China and regional tectonic movement [23,25,26]. From the late Pliocene, the depocenter of the Yangtze Delta and its adjacent area gradually moved southward in Figure 9. Accordingly, the Yangtze paleo-channel also moved southward from the North Jiangsu Basin to the estuarine area [45].

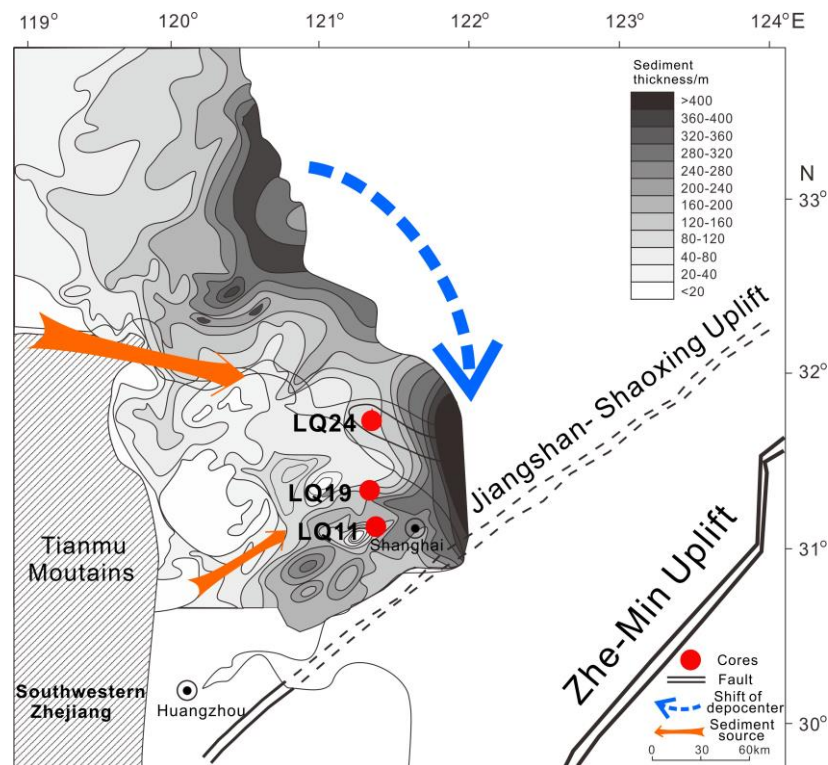


Figure 9. Sediment sources of the Yangtze Delta in the Quaternary. The contours of the sediment were modified after [45].

6. Conclusions

According to the analysis of detrital zircon morphology in core sediments of the Yangtze Delta, a change in the sediment provenance was detected at the Pliocene-Quaternary transition. In the Pliocene sediments, the morphology of detrital zircons with angular to subangular shapes and large elongation exhibited similar characteristics as those in the tributaries of the Lower Yangtze. It indicated that the Pliocene provenance was merely from the proximal (the Lower Yangtze and southwestern Zhejiang Province). However, the Quaternary strata documented different zircon morphologies. During this time, the zircon roundness and elongation matched well with samples from the Yangtze mainstream and the Middle Yangtze tributaries. For these samples, stubby, well-rounded zircon grains suggested that sediment provenance was extended to multiple sources in the distal Yangtze drainage. Sediments transported over long distances from the distal Yangtze basin finally reached the estuary area since the Quaternary. The morphology of detrital zircon has proven useful when studying source-to-sink dynamics of sediments.

Author Contributions: Conceptualization, W.Y.; Methodology, X.Y., J.S., and L.Z.; Resources, W.Y. and X.L.; Writing-Review & Editing, W.Y. and X.Y.

Funding: This work was financially supported by the National Natural Science Foundation of China (NSFC, No.: 41706048, 41730531), the Chinese Postdoctoral Science Foundation (No.: 2017M611611), A Project Funded by

the Priority Academic Program Development of Jiangsu Higher Education Institutions, and the Natural Science Foundation of Shandong Province, China (No.: ZR2019MD009).

Acknowledgments: We would like to give thanks to four anonymous reviewers for their constructive comments on this manuscript.

Conflicts of Interest: The authors declare no conflict of interest.

References

- Bianchi, T.S.; Allison, M.A. Large-river delta-front estuaries as natural “recorders” of global environmental change. *PNAS* **2009**, *106*, 8085–8092. [[CrossRef](#)]
- Bentley Sr, S.J.; Blum, M.D.; Maloney, J.; Pond, L.; Paulsell, R. The Mississippi River source-to-sink system: Perspectives on tectonic, climatic, and anthropogenic influences, Miocene to Anthropocene. *Earth Sci. Rev.* **2016**, *153*, 139–174. [[CrossRef](#)]
- Jin, B.F.; Wang, M.Y.; Yue, W.; Zhang, L.L.; Wang, Y.J. Heavy Mineral Variability in the Yellow River Sediments as Determined by the Multiple-Window Strategy. *Minerals* **2019**, *9*, 85. [[CrossRef](#)]
- Morton, A.C.; Hallsworth, C.R. Processes controlling the composition of heavy mineral assemblages in sandstones. *Sediment. Geol.* **1999**, *124*, 3–29. [[CrossRef](#)]
- Yang, S.Y.; Li, C.X.; Cai, J.G. Geochemical compositions of core sediments in eastern China: Implication for Late Cenozoic palaeoenvironmental changes. *Palaeogeogr. Palaeoclimatol. Palaeoecol.* **2006**, *229*, 287–302. [[CrossRef](#)]
- Gärtner, A.; Youbi, N.; Villeneuve, M.; Linnemann, U.; Sagawe, A.; Hofmann, M.; Zieger, J.; Mahmoudi, A.; Boumehdi, M.A. Palaeogeographic implications from the sediments of the Sebkhha Gezmayet unit of the Adrar Souttouf Massif (Moroccan Sahara). *Comptes Rendus Geosci.* **2018**, *350*, 255–266. [[CrossRef](#)]
- Garzanti, E.; Andò, S. Heavy Minerals for Junior Woodchucks. *Minerals* **2019**, *9*, 148. [[CrossRef](#)]
- Schoene, B.; Samperton, K.M.; Eddy, M.P.; Keller, G.; Adatte, T.; Bowring, S.A.; Khadri, S.F.R.; Gertsch, B. U-Pb geochronology of the Deccan Traps and relation to the end-Cretaceous mass extinction. *Science* **2015**, *347*, 182–184. [[CrossRef](#)]
- Fielding, L.; Najman, Y.; Millar, I.; Butterworth, P.; Garzanti, E.; Vezzoli, G.; Barfod, D.; Kneller, B. The initiation and evolution of the River Nile. *Earth Planet. Sci. Lett.* **2018**, *489*, 166–178. [[CrossRef](#)]
- Augustsson, C.; Voigt, T.; Bernhart, K.; Kreißler, M.; Gaupp, R.; Gärtner, A.; Hofmann, M.; Linnemann, U. Zircon size-age sorting and source-area effect: The German Buntsandstein Group. *Sediment. Geol.* **2018**, *375*, 218–231. [[CrossRef](#)]
- Morton, A.; Ellis, D.; Fanning, M.; Jolley, D.; Whitham, A. The importance of an integrated approach to provenance studies: A case study from the Paleocene of the Faroe-Shetland Basin, NE Atlantic. *Geol. Soc. Am. Spec. Pap.* **2012**, *487*, 1–12.
- Garzanti, E. From static to dynamic provenance analysis—Sedimentary petrology upgraded. *Sediment. Geol.* **2016**, *336*, 3–13. [[CrossRef](#)]
- Gärtner, A.; Linnemann, U.; Sagawe, A.; Hofmann, M.; Ullrich, B.; Kleber, A. Morphology of zircon crystal grains in sediments—characteristics, classifications, definitions. *Geol. Saxonica* **2013**, *59*, 65–73.
- Salata, D. Advantages and limitations of interpretations of external morphology of detrital zircon: A case study of the Ropianka and Menilite formations (Skole Nappe, Polish Flysch Carpathians). *Ann. Soc. Geol. Pol.* **2014**, *84*, 153–165.
- Zoleikhaei, Y.; Frei, D.; Morton, A.; Zamanzadeh, S.M. Roundness of heavy minerals (zircon and apatite) as a provenance tool for unraveling recycling: A case study from the Sefidrud and Sarbaz rivers in N and SE Iran. *Sediment. Geol.* **2016**, *342*, 106–117. [[CrossRef](#)]
- Gärtner, A.; Youbi, N.; Villeneuve, M.; Sagawe, A.; Hofmann, M.; Mahmoudi, A.; Boumehdi, M.A.; Linnemann, U. The zircon evidence of temporally changing sediment transport—The NW Gondwana margin during Cambrian to Devonian time (Aoucert and Smara areas, Moroccan Sahara). *Int. J. Earth Sci.* **2017**, *106*, 2747–2769. [[CrossRef](#)]
- Resentini, A.; Ando, S.; Garzanti, E. Quantifying roundness of detrital minerals by image analysis: Sediment transport, shape effects, and provenance implications. *J. Sediment. Res.* **2018**, *88*, 276–289. [[CrossRef](#)]

18. Miao, Y.F.; Zhang, P.; Lu, S.M.; Wu, X.Y.; Li, L.L.; Chen, H.G.; Li, X.Q.; Miao, Q.Y.; Feng, W.L.; Ou, J. Late Quaternary pollen records from the Yangtze River Delta, East China, and its implications for the Asian monsoon evolution. *Arab. J. Geosci.* **2015**, *8*, 7845–7854. [[CrossRef](#)]
19. Wang, Z.H.; Saito, Y.; Zhan, Q.; Nian, X.M.; Pan, D.D.; Wang, L.; Chen, T.; Xie, J.L.; Li, X.; Jiang, X.Z. Three-dimensional evolution of the Yangtze River mouth, China during the Holocene: Impacts of sea level, climate and human activity. *Earth Sci. Rev.* **2018**, *185*, 938–955. [[CrossRef](#)]
20. Fan, D.D.; Li, C.X. Timing of the Yangtze initiation draining the Tibetan Plateau throughout to the East China Sea: A review. *Front. Earth Sci.* **2008**, *2*, 302–313. [[CrossRef](#)]
21. Jia, J.T.; Zheng, H.B.; Huang, X.T.; Wu, F.Y.; Yang, S.Y.; Wang, K.; He, M.Z. Detrital zircon U-Pb ages of late Cenozoic sediments from the Yangtze Delta, Implication for the evolution of the Yangtze River. *Chin. Sci. Bull.* **2010**, *55*, 1520–1528. [[CrossRef](#)]
22. Liu, X.B. Magnetic properties of late Cenozoic sediments in south and north flanks of the Yangtze delta: Source-sink implications for river's connection to the sea. Ph.D. Dissertation, East China Normal University, Shanghai, China, 2017; pp. 43–47. (In Chinese with English abstract)
23. Liu, X.B.; Chen, J.; Maher, B.A.; Zhao, B.C.; Yue, W.; Sun, Q.L.; Chen, Z.Y. Connection of the proto-Yangtze River to the East China Sea traced by sediment magnetic properties. *Geomorphology* **2018**, *303*, 162–171. [[CrossRef](#)]
24. Huang, X.T.; Zheng, H.B.; Yang, S.Y.; Xie, X. Investigation of sedimentary geochemistry of core DY03 in the Yangtze Delta: Implication to tracing provenance. *Quat. Sci.* **2009**, *29*, 299–307. (In Chinese with English abstract)
25. Fan, D.D.; Li, C.X.; Yokoyama, K.; Zhou, B.C.; Li, B.H.; Wang, Q.; Yang, S.Y.; Deng, B.; Wu, G.X. Monazite age spectra in the Late Cenozoic strata of the Changjiang delta and its implication on the Changjiang run-through time. *Sci. China Ser. D Earth Sci. Engl. Ed.* **2005**, *48*, 171–1727. [[CrossRef](#)]
26. Yue, W.; Liu, J.T.; Zhang, D.; Wang, Z.H.; Zhao, B.C.; Chen, Z.Y.; Chen, J. Magnetite with anomalously high Cr₂O₃ as a fingerprint to trace upper Yangtze sediments to the sea. *Geomorphology* **2016**, *268*, 14–20. [[CrossRef](#)]
27. Yue, W.; Jin, B.F.; Zhao, B.C. Transparent heavy minerals and magnetite geochemical composition of the Yangtze River sediments: Implication for provenance evolution of the Yangtze Delta. *Sediment. Geol.* **2018**, *364*, 42–52. [[CrossRef](#)]
28. Chen, J.; Wang, Z.H.; Chen, Z.Y.; Wei, Z.X.; Wei, T.Y.; Wei, W. Diagnostic heavy minerals in Plio–Pleistocene sediments of the Yangtze Coast, China with special reference to the Yangtze River connection into the sea. *Geomorphology* **2009**, *113*, 129–136. [[CrossRef](#)]
29. Wang, Z.H.; Zhang, D.; Li, X.; Tao, S.K.; Xie, Y. Magnetic properties and relevant minerals of late Cenozoic sediments in the Yangtze River delta and their implications. *Geol. China* **2008**, *35*, 670–680. (In Chinese with English abstract)
30. Schneiderman, J.S.; Chen, Z.Y.; Eckert, J.O. Heavy minerals and river channel migration in the Yangtze delta plain, Eastern China. *J. Coast. Res.* **2003**, *19*, 326–335.
31. Changjiang Water Resources Commission. *Changjiang Sediment Bulletin in 2017*; Changjiang Press: Wuhan, China, 2017. (In Chinese)
32. He, M.Y.; Zheng, H.B.; Clift, P.D. Zircon U-Pb geochronology and Hf isotope data from the Yangtze River sands: Implications for major magmatic events and crustal evolution in Central China. *Chem. Geol.* **2013**, *360*, 186–203. [[CrossRef](#)]
33. Chen, Z.Y.; Li, J.F.; Shen, H.T.; Wang, Z.H. Yangtze River of China: Historical analysis of discharge variability and sediment flux. *Geomorphology* **2001**, *41*, 77–91. [[CrossRef](#)]
34. Ma, L.F.; Qiao, X.F.; Liu, N. *Geological Atlas of China*; Geological Publishing House: Beijing, China, 2002. (In Chinese with English abstract)
35. Wang, Z.J.; Chen, Z.Y.; Wei, Z.X.; Wang, Z.H.; Wei, T.Y. Coupling controls of neotectonism and paleoclimate on the Quaternary sediments of the Yangtze (Changjiang) coast. *Chin. Sci. Bull.* **2005**, *50*, 1775–1784. [[CrossRef](#)]
36. Deng, C.W.; Zhang, X.; Lin, C.M.; Xu, Z.Y.; Yu, J. Grain size analysis and environmental evolution indicated by the ZK01 borehole samples in the Changjiang delta since the latest glacial maximum. *Sediment. Geol. Tethyan Geol.* **2016**, *17*, 37–46. (In Chinese with English abstract)
37. Mange, M.A.; Maurer, H.F.W. *Heavy Minerals in Colour*; Chapman and Hall: London, UK, 1992; pp. 135–151.

38. Cox, E.P. A method of assigning numerical and percentage values to the degree of roundness of sand grains. *J. Paleontol.* **1927**, *1*, 179–183.
39. Powers, M.C. A new roundness scale for sedimentary particles. *J. Sediment. Res.* **1953**, *23*, 117–119. [[CrossRef](#)]
40. Poldervaart, A. Zircons in Rocks; 1. Sedimentary Rocks. *Am. J. Sci.* **1955**, *253*, 433–461. [[CrossRef](#)]
41. Poldervaart, A. Zircons in Rocks; 2. Igneous Rocks. *Am. J. Sci.* **1956**, *254*, 521–554. [[CrossRef](#)]
42. Osorio-Granada, E.; Restrepo-Moreno, S.A.; Muñoz-Valencia, J.A.; Trejos-Tamayo, R.A.; Pardo-Trujillo, A.; Barbosa-Espitia, A.A. Detrital zircon typology and U/Pb geochronology for the Miocene Ladrilleros-Juanchaco sedimentary sequence, Equatorial Pacific (Colombia): New constraints on provenance and paleogeography in northwestern South America. *Geol. Acta* **2017**, *15*, 201–215.
43. Pupin, J.P. Zircon and granite petrology. *Contrib. Mineral. Petr.* **1980**, *73*, 207–220. [[CrossRef](#)]
44. Corfu, F.; Hanchar, J.M.; Hoskin, P.W.O.; Kinny, P. Atlas of zircon textures. *Rev. Mineral. Geochem.* **2003**, *53*, 469–500. [[CrossRef](#)]
45. Chen, Z.Y.; Stanley, D.J. Quaternary subsidence and river channel migration in the Yangtze Delta plain, Eastern China. *J. Coast. Res.* **1995**, *11*, 927–945.
46. Yue, W.; Yang, S.Y.; Zhao, B.C.; Chen, Z.Y.; Yu, J.J.; Liu, X.B.; Huang, X.T.; Jin, B.F.; Chen, J. Changes in environment and provenance within the Changjiang (Yangtze River) Delta during Pliocene to Pleistocene transition. *Mar. Geol.* **2019**, *416*, 105976. [[CrossRef](#)]
47. Fedo, C.M.; Sircombe, K.N.; Rainbird, R.H. Detrital zircon analysis of the sedimentary record. *Rev. Mineral. Geochem.* **2003**, *53*, 277–303. [[CrossRef](#)]
48. Nie, J.S.; Horton, B.K.; Saylor, J.E.; Mora, A.; Mange, M.; Garziona, C.N.; Basu, A.; Moreno, C.J.; Caballero, V.; Parra, M. Integrated provenance analysis of a convergent retroarc foreland system: U-Pb ages, heavy minerals, Nd isotopes, and sandstone compositions of the Middle Magdalena Valley basin, northern Andes, Colombia. *Earth Sci. Rev.* **2012**, *110*, 111–126. [[CrossRef](#)]
49. Cascalho, J. Provenance of Heavy Minerals: A Case Study from the WNW Portuguese Continental Margin. *Minerals* **2019**, *9*, 355. [[CrossRef](#)]



© 2019 by the authors. Licensee MDPI, Basel, Switzerland. This article is an open access article distributed under the terms and conditions of the Creative Commons Attribution (CC BY) license (<http://creativecommons.org/licenses/by/4.0/>).